NMR Chemical Shift Perturbation Study of the N-Terminal Domain of Hsp90 upon Binding of ADP, AMP-PNP, Geldanamycin, and Radicicol

ARTICLE *in* CHEMBIOCHEM · SEPTEMBER 2003

Impact Factor: 3.09 · DOI: 10.1002/cbic.200300658 · Source: PubMed

6 AUTHORS, INCLUDING:

Julien Furrer
Universität Bern
81 PUBLICATIONS **1,119** CITATIONS

SEE PROFILE

Klaus Richter
Technische Universität München
75 PUBLICATIONS **3,436** CITATIONS

SEE PROFILE

NMR Chemical Shift Perturbation Study of the N-Terminal Domain of Hsp90 upon Binding of ADP, AMP-PNP, Geldanamycin, and Radicicol**

Alexander Dehner, Julien Furrer, Klaus Richter, Ioana Schuster, Johannes Buchner, and Horst Kessler*[a]

Hsp90 is one of the most abundant chaperone proteins in the cytosol. In an ATP-dependent manner it plays an essential role in the folding and activation of a range of client proteins involved in signal transduction and cell cycle regulation. We used NMR shift perturbation experiments to obtain information on the structural implications of the binding of AMP-PNP (adenylyl-imidodiphosphate—a non-hydrolysable ATP analogue), ADP and the inhibitors radicicol and geldanamycin. Analysis of $^{1}H,^{15}N$ correlation spectra showed a specific pattern of chemical shift perturbations at N210 (ATP binding domain of Hsp90, residues 1–210) upon ligand binding. This can be interpreted qualitatively either as a consequence of direct ligand interactions or of ligand-induced conformational changes within the protein. All ligands show specific interactions in the binding site, which is known from the crystal structure of the N-terminal domain of Hsp90. For AMP-PNP and ADP, additional shift perturbations of residues outside the binding pocket were observed and can be regarded as a result of conformational rearrangement upon binding. According to the crystal structures, these regions are the first α-helix and the "ATP-lid" ranging from amino acids 85 to 110. The N-terminal domain is therefore not a passive nucleotide-binding site, as suggested by X-ray crystallography, but responds to the binding of ATP in a dynamic way with specific structural changes required for the progression of the ATPase cycle.

KEYWORDS:

ATPase · chaperone proteins · inhibitors · NMR spectroscopy · protein–ligand interactions · protein structures

Introduction

The molecular chaperone Hsp90 is known to assist a specific set of substrates, such as steroid hormone receptors and tyrosine kinases, in achieving suitable conformations.[1–4] The mechanism of this reaction is poorly understood, but recent studies have indicated that the hydrolysis of ATP by the N-terminal domain of Hsp90 is necessary to perform this task in vivo.[5–7] Hsp90 functions as a dimeric protein with a dimerization domain localized at the very C-terminal end of the C-terminal domain. It has been shown that N-terminal fragments of Hsp90 are monomeric and that ATP does not alter the oligomerization behaviour of these fragments.[8] In contrast, ATP binding to full-length Hsp90 leads to a transient dimerization of the N-terminal domains and their association with the middle domain, followed by stimulation of ATPase activity.[8, 9] This N-terminal dimerization is achieved by a "strand swapping" mechanism, involving the first 24 amino acids of the N-terminal domain.[10] The N-terminal ATP-binding domain was subsequently found to have homology to other related ATPases such as Gyrase B and MutL[11] and thus these proteins were grouped into the superclass of GHKL-ATPases (**G**yrase, **H**sp 90, **K**inase, Mut**L**, histidine kinase CheA).[12] The ATPase activity of Hsp90 can be inhibited by natural substances such as geldanamycin and radicicol, which bind to the nucleotide binding site with high affinity. Binding of these inhibitors to Hsp90 has been shown to revert the tumour phenotype of *src*- and *ras*-related oncogenic growth.[13, 14] This is accomplished by the release of substrates from the inhibited Hsp90 and subsequent degradation of at least some of these proteins.[15–17]

Hsp90 is known to undergo large conformational changes during the ATPase cycle, involving the C-terminal regions of the ATP-binding site,[18, 19] which are also required for efficient progress of the ATPase reaction. The movements undergone during the ATPase cycle of Hsp90 seem to be important for the interaction of partner proteins and the chaperoning of substrate proteins.

At present, X-ray crystallographic structures of the N-terminal nucleotide-binding domain from yeast and human Hsp90 in complexation with ADP, ATP, radicicol, and geldanamycin are known.[7, 20, 21] All ligands have been shown to bind in a deep

[a] *Prof. Dr. H. Kessler, Dipl. Chem. A. Dehner, Dr. J. Furrer, Dr. K. Richter, I. Schuster, Prof. Dr. J. Buchner*
Technische Universität München
Institut für Organische Chemie und Biochemie
Lichtenbergstrasse 4, 85747 Garching (Germany)
Fax. (+49) 89-289-13210
E-mail: Kessler@ch.tum.de

[**] *AMP-PNP, adenylyl-imidodiphosphate.*

  DOI: 10.1002/cbic.200300658

pocket made up of two α-helices with the central β-sheet as its base. For ATP and ADP, the nucleotide adopts a unique kinked conformation not observed for any other type of ATP-binding protein. In this conformation, the γ-phosphate points outside the protein, and is the only solvent-accessible part of the nucleotide. Unexpectedly, in crystal structures of the N-terminal domains, ligand binding did not result in detectable conformational changes.[7, 20, 21]

To gain insight into the different effects of ligand binding to the N-terminal domain of Hsp90 (N210, residues 1 – 210), we compared the chemical shift perturbation patterns of the N-terminal domain in complexation with ADP, adenylyl-imidodiphosphate (AMP-PNP, a non-hydrolysable ATP analogue), [9] radicicol, and geldanamycin by NMR spectroscopy. Our results show that ligand binding results in specific chemical shift patterns of the residues within the binding pocket and in surrounding regions, which can be assigned to distinct direct interactions or conformational rearrangements.

Results

To analyse the consequences of ligand binding of the N-terminal domain of Hsp90 we initially assigned the ^{1}H, ^{13}C, and ^{15}N backbone resonances of the free $^{2}H/^{13}C/^{15}N$-labelled N210 protein by a set of triple resonance experiments (see Experimental Section). All assignments have been confirmed by a recently published backbone signal assignment of a Hsp90 construct comprising amino acids 1 to 207.[22] This provided the basis for analysis of the interaction of ATP, ADP and the competitive inhibitors geldanamycin and radicicol with N210. The $^{1}H,^{15}N$-correlation spectrum of a protein and its specific pattern can be regarded as a fingerprint of its structure. Changes in resonance frequencies of individual nuclei are due to different electronic and/or conformational environments. Perturbations of ^{15}N and H^{N} chemical shifts of a protein upon complexation with a ligand are a qualitative tool for mapping of residues involved in binding sites and/or identifying conformational rearrangements.[23–26] However, there is no quantitative correlation of the size of the induced shift with the strength of binding or the conformational rearrangement. In addition, complete disappearance of peaks can occur upon complexation, and this has to be taken into account when analysing the data. Since these effects can extend beyond the binding site, a comparison of the chemical shifts of all cross-peaks in the presence and in the absence of ligands is required for correct definition of the area of the protein directly involved in binding and those only indirectly perturbed as a result of conformational rearrangements.

In Figure 1 we show a superposition of the $^{1}H,^{15}N$ HSQC[27] of free N210 (red contours) and ADP-bound N210 (blue contours). Titration of N210 with ADP (also with AMP-PNP, radicicol, and geldanamycin; data not shown) produced severe shifts in several cross-peaks in the $^{1}H,^{15}N$ HSQC spectrum, while the large majority of peaks were rather slightly affected. Because of the strong binding constants of the nucleotides and the inhibitors, the complexes are long-lived on the NMR chemical shift timescale ($\tau > 10$ ms), which resulted in the production of a

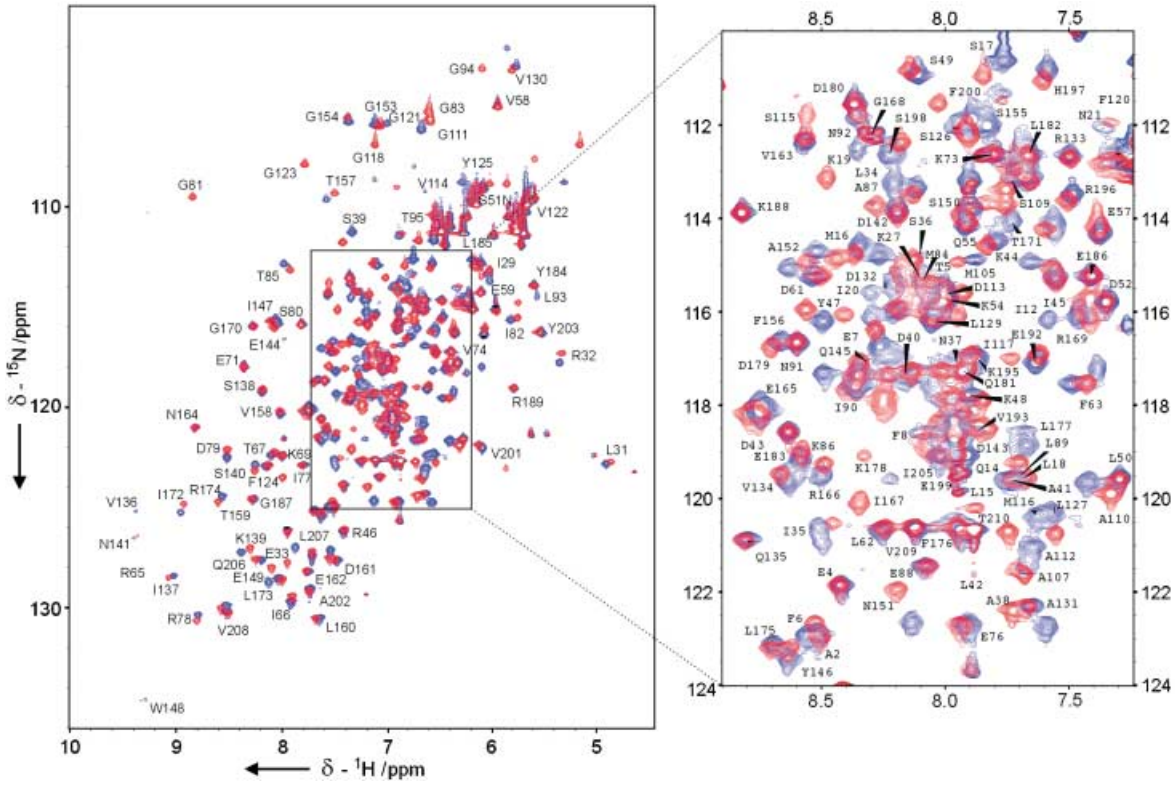

Figure 1. *Superposition of the $^{1}H,^{15}N$ HSQC spectra of free N210 (red contours) and N210/ADP complex (blue contours) with an expanded view recorded on a Bruker spectrometer (750 MHz ^{1}H frequency). Cross-peaks are labelled at their position in the free N210 (red). Both samples contained approximately 550 μM Hsp90 in 40 mM phosphate buffer (pH 7.5) in 90% H_2O/10% D_2O. Spectra were recorded at 298 K.*

second signal set, instead of a progressive signal shifting during the titration experiments. It is therefore not possible to trace the signals from the free state to the complexed state as is feasible for binders of lower affinity. A classical assignment would have required a set of triple resonance experiments and triple-labelled N210 for each ligand complex. Because of the low sample stability, we decided to use a different strategy,[28] in which chemical shift perturbations of the N210 complexes were determined through the *minimum deviation* between each position of the free and the complexed peak in the $^{1}H,^{15}N$ HSQC spectra.[28] Using the disappearance of a signal and by identifying the next neighbour we determine the minimal induced shift due to complexation of each residue.

To prevent chemical shift changes because of fast hydrolysis of ATP to ADP in the $^{1}H,^{15}N$ correlation spectra we used the non-hydrolysable AMP-PNP for the perturbation experiments.[9] In Figure 2, changes in chemical shifts are displayed through the use of the normalised weighted chemical shift average[29] Δ_{av} between the free N210 and its complex with AMP-PNP, ADP, radicicol, and geldanamycin. Titration of all four ligands to ^{15}N-labelled Hsp90 caused significant chemical shift perturbations and disappearance of individual resonances in the $^{1}H,^{15}N$ HSQC spectra, while the chemical shifts of the remaining signals were affected only slightly or not at all.

The results for the AMP-PNP ligand are depicted in Figure 2a. Three defined regions show severe chemical shift changes. The first is situated in the so-called binding pocket of Hsp90 (Figure 3), which, according to the crystal structure determined for the N210/ATP complex, is the main interaction surface of the protein.[7] The largest chemical shift perturbations can be found for residues Gly81, Gly83, Asn92, Leu93, Gly94, Ile117, Gly118, Gly121, Val122, and Gly123, as well as the peaks of Ile77 and Ile96, which could not be followed upon complexation. The second region perturbed as a result of AMP-PNP binding is the very N-terminal part encompassing the first (Ala10 – Thr22) and the second (Glu28 – Leu50) α-helices, which surround the central binding pocket. In these helices, Ala12, Leu15, Ser17, Ile20, Arg32, Glu33, Ala38, Ser29, Ala41, and Lys44 show significant shift changes, whereas the signal for Asn21 could not be followed. The third region is situated in the β-sheets forming the C-terminal part (150 – 210) of N210 and the base of the binding pocket (residues Ile77, Asp79, Val136, Ser138, Thr171, and Ile173; Figure 3). In particular, residues Glu144, Asn151, Ser155, Ile172, Leu173, Lys178, and Lys191 show significant shift perturbations, whereas the signal for Ile167 completely disappears.

The results for the ADP-N210 complex are presented in Figure 2b. Despite localised differences, the overall chemical shift perturbation pattern is similar to that described above for the AMP-PNP complex, not unexpected in view of the very similar chemical structures of the nucleotides. The largest chemical shift changes due to complexation are localized in the binding pocket and in the surrounding N-terminal α-helices (Ala10 – Thr22, Glu28 – Leu50) and C-terminal β-sheets (Arg133 – Lys139, Tyr146 – Pro150, Ser155 – Leu160, and Gly170 – Leu177). The signals for residues Asn21, Glu28, and Ser36 in the first α-helix and for Glu144 and Thr157 in the C-terminal part could not be followed upon ligand binding. Significant differences between AMP-PNP and ADP binding occur for residue Gly121, which is strongly affected upon AMP-PNP binding, and residues Asn21, Thr85, and Leu93, which are more perturbed upon ADP binding.

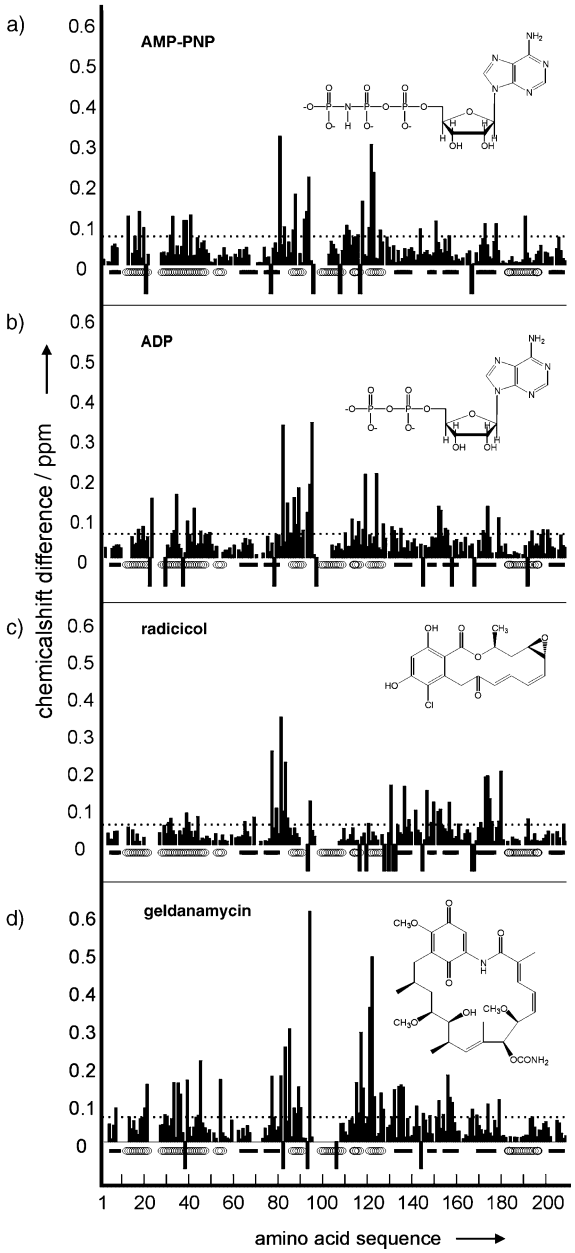

Figure 2. *Average chemical shift perturbation of ^{1}H and ^{15}N chemical shifts of N210 given by $\Delta_{av} = [(\Delta\delta^2_{NH} + \Delta\delta^2_{N}/25)/2]^{1/2}$ [ppm] against residue number upon titration with: a) AMP-PNP, b) ADP, c) radicicol, and d) geldanamycin. Negative bars indicate amino acids that could not be unambiguously assigned in the ligand complex. The secondary structure is given by bars indicating a β-strand and circles indicating a helix. Dotted lines represent the lower boundary for colour coding in Figure 5.*

The results for the radicicol – N210 complex are shown in Figure 2c. The overall chemical shift perturbation map is different from that described above for AMP-PNP and ADP, which indicates that radicicol binding leads to different effects within the ATP binding domain of Hsp90. While some residues—

namely, Ile77, Gly81, Ile82, Gly83, Asn92, and Gly93—show strong chemical shift perturbations, the overall binding pocket is less affected by radicicol binding than in the cases of AMP-PNP and ADP. In addition, the shift changes observed within the two surrounding α-helices (Ala10 – Thr22, Glu28 – Leu50) remain rather weak. In contrast, the residues belonging to the Ser126 – Asp132 loop region and the four β-sheets (Arg133 – Lys139, Tyr146 – Pro150, Ser155 – Leu160, and Gly170 – Leu177) forming the base of the binding pocket are more strongly affected.

Of the four discussed ligands, the strongest chemical shift perturbations overall were induced by geldanamycin (Figure 2d). The shift changes within the binding pocket are large, the signals of residues Gly94, Gly121, and Val122 being especially strongly affected. In addition, the signals of Ile82 and Asn92 could not be followed, which is not the case for AMP-PNP, ADP, and radicicol binding. Similarly to AMP-PNP and ADP complexation, the shift differences for the residues within the two surrounding α-helices (Ala10 – Thr22, Glu28 – Leu50) are strongly affected and the signal for Ala39 is completely absent. The residues in the β-sheet belonging to the base of the binding pocket (Arg133 – Lys139, Tyr146 – Pro150, Ser155 – Leu160, and Gly170 – Leu177), however, are perturbed in a manner similar to that produced by radicicol binding.

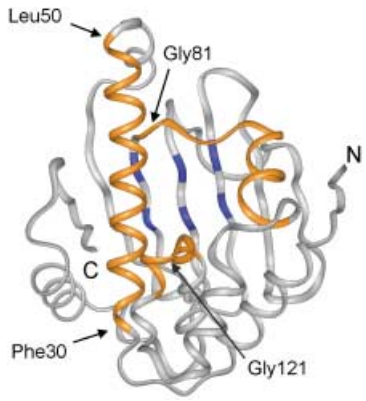

Figure 3. *Ribbon representation of the binding pocket of Hsp90. Residues in orange represent the helices 28 – 50 and 85 – 94, and the loops 117 – 124 and 81 – 85. Residues in blue are residues 77, 79, 136, 138, 171, and 173 in the base-forming β-sheet.*[7]

Discussion

The binding of ATP to the N-terminal domain of Hsp90 marks the beginning of the ATPase cycle, which results in the hydrolysis of the nucleotide through a coordinated series of conformational changes.[19] These changes involve as a critical transient state a conformation in which the N-terminal domains dimerize in the presence of ATP—and also in that of AMP-PNP.[2, 8, 9, 30] In this state, it is speculated that at least a part of the N-terminal α-helix is swapped from one N-terminal domain to the other.[10] Furthermore, the ATP molecule becomes trapped inside the protein, possibly by interactions of the N-terminal with the central domain.[19] These conformational changes require ligand-specific behaviour of the ATP-binding domain that cannot be explained on the basis of the crystal structures in the complexed state, since no differences in the conformation relative to the free state were observed.[7, 20]

The purpose of the NMR data presented here is to explore the ligand-binding site and additional conformational effects of the N-terminal domain of Hsp90 due to binding of AMP-PNP, ADP, radicicol, and geldanamycin. Chemical shift perturbations are a qualitative tool with which to detect changes in the electronic environments of specific nuclei that could result either from a direct ligand interaction or from a conformational rearrangement around the observed nuclei. Mapping of these sites onto the three-dimensional structure of N210 determined by X-ray crystallography (Figure 3) provides the structural basis for the described chemical shift perturbations. Significant shift deviations of signals belonging to residues not coincident with the binding site can be interpreted as conformational flexibility induced by ligand binding (Figure 4). Even though all four ligands are known to bind to the same site of the protein in competition with each other, the effects on the N-terminal domain of Hsp90 are different. The front and back views of N210 displayed in Figure 5 use colour-coding to denote amino acids significantly affected upon binding of AMP-PNP, ADP, radicicol, and geldanamycin. As expected, the strongest induced chemical shift changes for all four ligand complexes occur within and around the binding pocket. In particular, the loop 81 – 85, the helix 85 – 94 and the loop 117 – 124 are most strongly affected, being in direct contact with the ligands. In

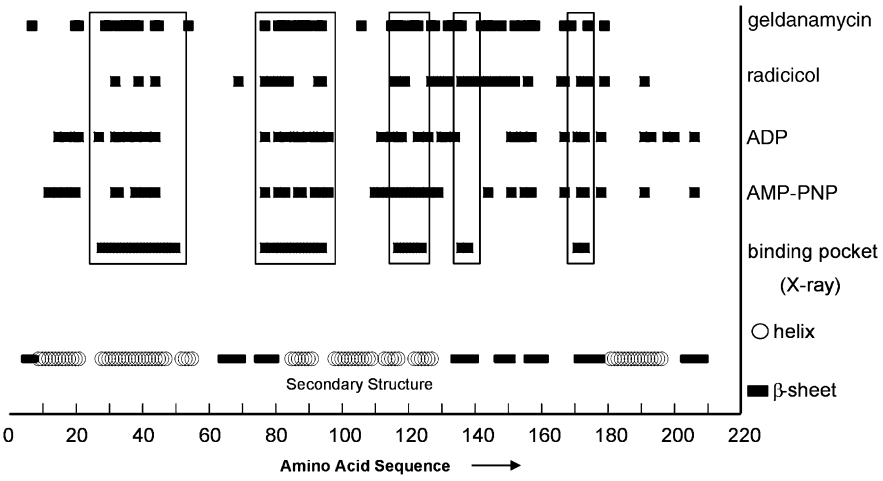

Figure 4. *Comparative representation of relative chemical shift perturbations (normalised as $\Delta_{av}/\Delta_{max} = 1.0$ for each ligand) larger than $\Delta_{av} > 0.2$ for AMP-PNP, ADP, and radicicol and $\Delta_{av} > 0.11$ for geldanamycin upon ligand binding versus residue number. Chemical shift perturbations within the binding pocket are indicated by a box. The secondary structure is given by bars indicating a β-strand and circles indicating a helix.*

addition, it is likely that these flexible loops undergo a conformational rearrangement and thus experience stronger chemical shift changes upon ligand binding. Located just between the β2 strand and the so-called "ATP-lid" region (residues 85 – 110), residues Gly81, Val82, and Gly83 are significantly perturbed upon binding of each ligand. The backbone amide of residue Gly83 had been shown to be involved in water-bridged hydrogen bonds with each ligand.[20] These residues belong to the "ATP-lid", which is a part of the nucleotide binding motif common within the gyrase, Hsp90, histidine kinase, MutL (GHKL) superfamily.[11] At the end of the α′ helix of this "ATP-lid", the signals of residues Asn92, Val93, and Gly94 show stronger chemical shift perturbations, especially for the titration with AMP-PNP and ADP. In particular, the side chain carbonyl of Asn92 had been shown to make direct contacts with O2′ of the ribose sugar of ATP and ADP.[20] In contrast, the radicicol and geldanamycin complexes do not display strong chemical shift deviations for these residues (except for Gly94 in the case of geldanamycin). This is in agreement with the crystal structures, in which neither inhibitor is involved in direct contacts with Asn92, Val93, or Gly94.[20] The L4 loop (residues 95 – 102)[9, 11] of this ATP-lid region remains completely invisible in the NMR spectra and could not even be assigned in the free N210 protein, indicating a millisecond-timescale flexibility. Taken together, our results confirm that this loop region is subject to conformational rearrangements upon binding of AMP-PNP, ADP, and geldanamycin. Another ligand-specific perturbation can be observed for residues Gly121, Val122, and Gly123, which are also strongly affected only upon binding of AMP-PNP, ADP, and geldanamycin. Figure 6 illustrates a ribbon representation of this region, showing the localizations and orientations of ADP, radicicol, and geldanamycin. With regard to the conformation and the smaller size of ADP, it is likely that the additional γ-phosphate group of bound ATP is involved in water-bridged contacts with these residues, in particular with the carbonyl group of Gly121 and the amide proton of Gly123. These direct interactions are reproduced by geldanamycin, with HN of Gly123 strongly bonding to the macrocycle,[20] whereas the smaller radicicol ligand is directed away from this loop region and therefore exhibits weaker direct interactions with these three residues.

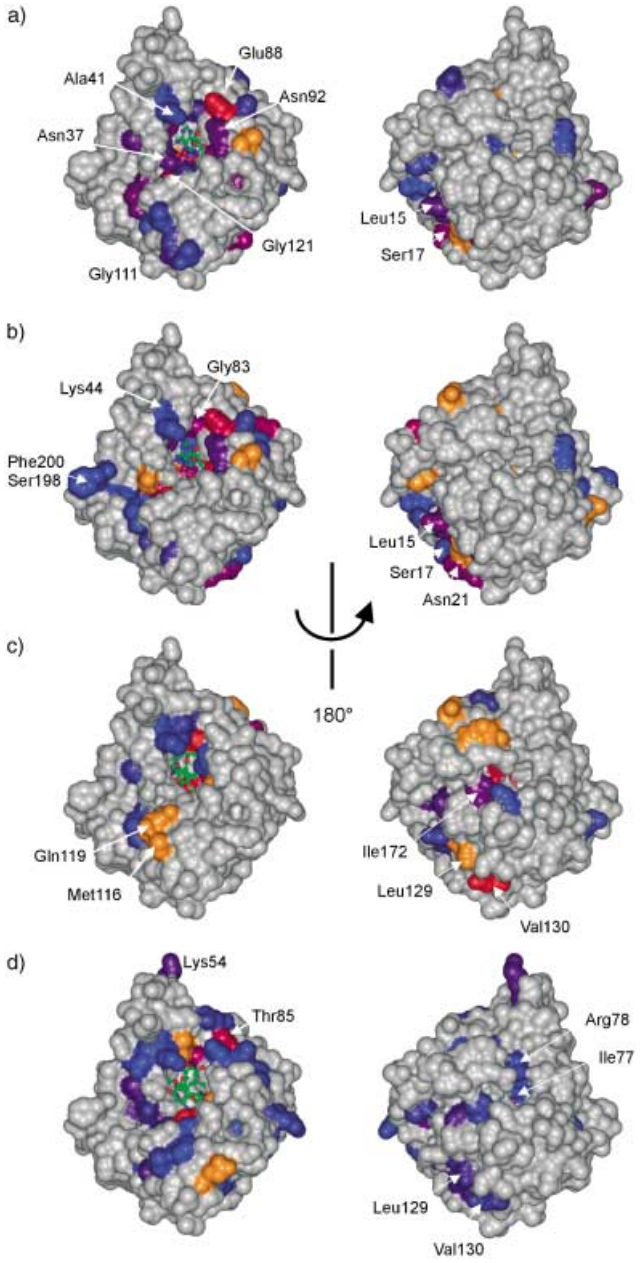

Figure 5. *Residues affected by chemical shift perturbation, mapped onto the crystal structure of Hsp90 by use of a Connolly surface with a probe radius of 1 Å. a) Titration with AMP-PNP, b) with ADP, c) with radicicol, and d) with geldanamycin. The relative orientation of the protein is identical to the ribbon diagram shown in Figure 3. The residues are coloured according to the following scheme: residues with a relative chemical shift perturbation (normalised as* $\Delta_{av}/\Delta_{max} = 1.0$ *for each ligand) smaller than twice the overall average (0.11 in the case of geldanamycin and 0.20 for AMP-PNP, ADP, and radicicol) are not significantly shifted, and are colour-coded in grey. Residues with relative chemical shift perturbations larger than 0.60 are shown in red. Residues with relative chemical shift perturbations between 0.20 and 0.60 are given from blue to red. Residues which are missing in the complexed spectrum or which could not be unambiguously assigned are shown in orange (negative bars in Figure 2). Residues Gly94, Gly81, Gly123, and Val122 are within the binding pocket and therefore buried by the solid surface.*

Several residues belonging to the base of the binding pocket (residues 138 – 178) are significantly affected upon complexation by each ligand (Figure 4). Especially, residues Val136, Ser138, Thr171, and Ile173 are particularly affected upon radicicol complexation. Because of its smaller size, it seems to insert more deeply into the binding pocket, which is consistent with the crystal structure of radicicol-complexed N210.[20] Residues Ile77 and Asp79 are also part of the binding pocket base. The interaction of the exocyclic ATP/ADP N6-amino group with the carboxyl side chain of Asp79 has been shown to be critical for the function of Hsp90 in vivo.[5, 6] Mutation of Asp79 to Asn is sufficient to abolish ATP-binding. Our results show that the backbone amide group of Asp79 is perturbed by this interaction with AMP-PNP, ADP, and with radicicol. Even though binding of geldanamycin resembles the binding of nucleotides[20]—as it has been observed that very similar residues are involved in the binding reaction—the chemical shift perturbation of Asp79 backbone amide upon geldanamycin binding is not pronounced.

The long α2 helix (Glu28 – Leu50) flanking the binding pocket is also affected upon binding of AMP-PNP, ADP, and geldana-

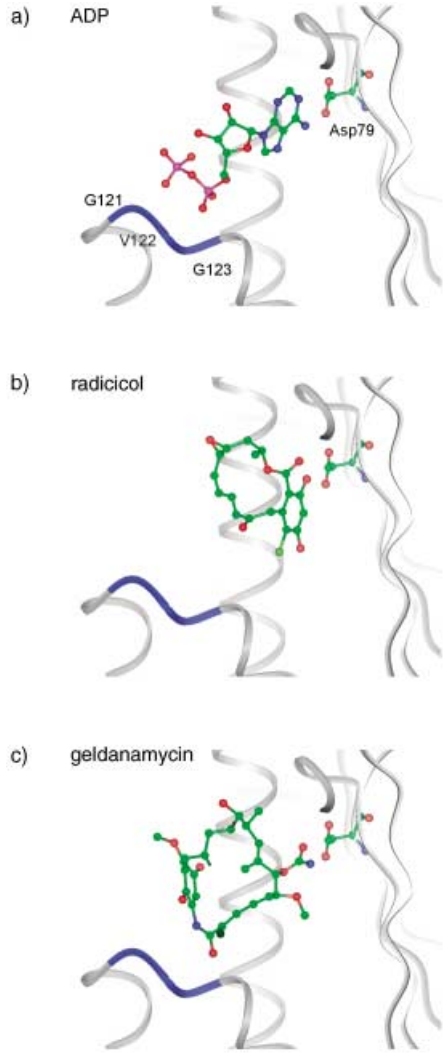

Figure 6. *Localization of ADP (a), radicicol (b), and geldanamycin (c) within the binding pocket with respect to the loop 117 – 124 according to the crystal structures. Viewed perpendicular to Figure 3. Ribbon representation in blue is given for residues Gly121, Val122, and Gly123. In addition, residue Asp79 in the β-sheet is displayed for orientation.*

mycin. In particular, this helix contains residues, such as Glu33, critical for the catalysis reaction. It is therefore likely that residues in this helix form direct contacts with the bound nucleotides. Mutation of Glu33 to Ala reduces the catalytic efficiency of full-length Hsp90 to undetectable levels, but still allows efficient binding of nucleotides.[5, 18] The distinct perturbation effects of AMP-PNP, ADP, and geldanamycin on this helix again highlight the similarity between geldanamycin binding and nucleotide binding. In contrast, the effect of radicicol on this helix is much less pronounced, which confirms that radicicol penetrates more deeply into the binding pocket.

Another interesting structural element is the first helix α1 (Ala10 – Thr22) of the protein. Although its chemical shift deviations are not pronounced, this helix merits attention, as it has been suspected to form a flexible structure that may be involved in a "strand-swapping" reaction between the two N-terminal domains during the ATP-hydrolysis reaction.[10] Specific chemical shift perturbations could be detected for residues situated in this first α-helix (Ile12, Leu15, Ser17, Ile19, and Ile20) upon binding of AMP-PMP, ADP, and geldanamycin. The crystal structure[7] of the domain suggests that these residues are involved in conformational rearrangements together with the loop region 90 – 103, which is also strongly affected upon binding of AMP-PNP, ADP, and geldanamycin (but not radicicol). As deletion of the first 24 amino acids does not affect nucleotide binding to the N-terminal domain,[10] direct involvement of these residues can be ruled out, so it is likely that the observed chemical shift deviations of these residues are the result of different chemical environments and therefore of ligand-induced conformational changes.

The large degree of similarity in the patterns of the chemical shift changes of AMP-PNP and ADP binding suggests that they have similar—though not identical—effects on the structure of the domain. Clear differences in chemical shift perturbations between AMP-PNP and ADP can only be observed for Gly121, Val122, and Gly123, which may be explained by the presence or absence of a water-bridged hydrogen bond. This observation may point to additional effects of the other domains of Hsp90, which have been suspected to make contact with the exposed γ-phosphate residue of the ATP.[19]

The differences in chemical shift perturbations upon ligand binding reported in this study add to our understanding of the conformational effects induced by AMP-PNP, ADP and the competitive inhibitors in the N-terminal domain of Hsp90. Ligand-specific internal dynamics may be transferred to the C-terminal domain of Hsp90 and thereby control its functionality. Taken together, our results imply that binding of ATP to the N-terminal domain of Hsp90 affects the conformation in a specific way. In the light of biochemical data,[8, 9] it is reasonable to assume that these changes are necessary for subsequent domain interactions in the Hsp90 molecule, linking ATP hydrolysis to a coordinated sequence of conformational changes required for assisting protein folding.

Experimental Section

Protein purification and sample preparation

The N-terminal domain of Hsp90, consisting of the amino acids 1 to 210, was purified from the *E. coli* strain BL21 (DE3) carrying the plasmid pET11a – N210.[31] The bacteria were grown in M9-medium (minimal growth medium)[39] containing ^{15}N-labelled NH_4Cl (Cambridge Isotope Laboratories, Andover, USA) as the sole nitrogen source. For preparation of ^{13}C-labelled protein, $^{13}C_6$-glucose (Cambridge Isotope Laboratories, Andover, USA) was used as sole carbon source. Bacteria were grown to an OD_{600} of about 0.5. Protein induction was then started with the addition of isopropyl-β-D-thiogalactopyranoside (IPTG, 1.5 mM) and continued overnight at 30 °C. Protein purification was achieved as described previously.[31] In brief, column chromatography on a DEAE-Sephadex column (Amersham Biosciences, Uppsala, Sweden) was used as first purification step. The protein was then dialysed against potassium phosphate (40 mM, pH 7.0) and applied to column chromatography on a hydroxyapatite column. The flow through was further purified by use of a Resource Q-column and a Superdex 75 PrepGrade

(Amersham Biosciences, Uppsala, Sweden). The eluted protein was concentrated and dialysed against potassium phosphate (40 mM, pH 7.5), which was the buffer used for the NMR experiments.

The $^{2}H/^{13}C/^{15}N$-labelled protein was purified by the same procedure, except that the bacterial growth was performed in 1 L LB_0 medium (luria broth)[39] until an OD_{600} of about 1.5 was obtained. The cells were spun down and resuspended in M9 medium containing $^{15}NH_4Cl$, $^{13}C_6$-glucose and 70% D_2O (Cambridge Isotope Laboratories, Andover, USA). Bacterial growth was continued at 37 °C until the OD_{600} had doubled once, and IPTG (1.5 mM) was added thereafter. Protein expression was performed at 30 °C overnight.

Samples for the NMR experiments were concentrated to about 550 μM N210. Geldanamycin was a kind gift from the Experimental Drug Division (NIH, Bethesda, USA). Radicicol was obtained from Sigma, while AMP-PNP and ADP were from Roche Applied Sciences (Mannheim, Germany).

NMR spectroscopy

For the sequential assignment of the N-terminal domain of Hsp90, a uniformly $^{15}N/^{13}C/^{2}H$-labelled (80%) sample (40 mM phosphate buffer, pH 7.5) in H_2O/D_2O (9:1) with a concentration of 800 μM N210 was used. All NMR spectra were acquired at 303 K on a Avance Bruker spectrometer (800 MHz ^{1}H frequency) equipped with a four-channel probe and triple axis gradients. The assignments of ^{1}H, ^{15}N, ^{13}CO, $^{13}C\alpha$, and $^{13}C\beta$ chemical shifts were determined by a series of TROSY-type triple resonance experiments with ^{2}H decoupling: HNCO, HNCA, HN(CO)CA, HN(CA)CO, and a HN(CO)CACB.[32, 33] All the experiments were processed and analysed by use of Xwin-NMR 3.5 and Aurelia 3.5. Sequence-specific resonance assignments were obtained with the assignment program PASTA.[34] The obtained backbone assignment independently confirms the recently published assignment.[22]

The titration experiments were performed with uniformly ^{15}N-labelled N210 by use of four 600 μL samples (550 μM protein, 40 mM potassium phosphate buffer, pH 7.5, 10% $^{2}H_2O$), at 298 K, on a Bruker Avance spectrometer (750 MHz ^{1}H frequency) equipped with a four-channel probe and triple axis gradients. The backbone assignment deposited in the BioMagResBank (accession number 5355)[22] could be completely transferred onto our spectra, which exhibit only slight chemical shift changes for the amide resonances, owing to different sample preparation strategies. The $^{1}H,^{15}N$ HSQC spectra were obtained by the fast-HSQC method,[27] in order to obtain a suitable signal to noise ratio for the water-exchangeable amide protons and good water suppression, which was carried out by use of the WATERGATE sequence.[35, 36] A total of 2048 complex points in t_2 with 512 t_1 increments was acquired, with 16 scans for each increment. The spectral width used was 12.818 ppm for ^{1}H and 39.15 ppm for ^{15}N. The NMR data were processed with the Bruker program package XWin-NMR Version 3.5 and Sparky Version 3.106.[37, 38] Zero-filling, Gaussian (t_2) and 90° shifted sine-bell apodisation (t_1) were applied prior to Fourier transformations, and subsequent baseline corrections were performed in both dimensions.

Titration experiments

The titration experiments were carried out with the non-hydrolysable AMP-PNP instead of ATP. For AMP-PNP and ADP an aqueous solution (50 mM) was prepared in potassium phosphate buffer (40 mM, pH 7.5, 100 mM Mg^{2+}). The ligands were added to a 550 μM solution of ^{15}N-labelled N210, and a series of $^{1}H,^{15}N$ HSQC spectra were recorded at various ligand concentrations in the 0–2.26 mM range in the case of AMP-PNP (0–96% bound complex; K_d(AMP-PNP) ≈ 70 μM) and 0–4.64 mM for ADP (0–99% bound complex; K_d(ADP) ≈ 10 μM).[10] The competitive inhibitors radicicol and geldanamycin were each dissolved to form a solution in $[D_6]$DMSO (60 mM). Prior to titration of the inhibitors, a single reference $^{1}H,^{15}N$ HSQC of the free N210 sample was recorded, to which 1% $[D_6]$DMSO was added. A series of $^{1}H,^{15}N$ HSQC spectra were subsequently recorded with use of increasing concentrations of radicicol (0–0.8 mM; K_d(radicicol) ≈ 0.9 nM) and geldanamycin (0–0.6 mM; K_d(geldanamycin) ≈ 1.2 μM). Because of the binding constants of AMP-PNP, ADP, and the inhibitors ($K_d < 100$ μM), the complexes were long-lived on the NMR chemical shift timescale ($\tau > 10$ ms). Accordingly, a second signal set for the ligand-complexed N210 appeared during the titration. Chemical shift perturbations of the N210 complexes were determined from the minimum deviation between each position of the free and the complexed peak in the $^{1}H,^{15}N$ HSQC spectra.[28] For analysis of the chemical shift perturbations of ^{1}H and ^{15}N backbone resonances, a weighted average chemical shift change given by

$$\Delta_{av} = \sqrt{(\Delta\delta_{NH}^2 + \Delta\delta_N^2/25)/2} \quad (1)$$

was calculated and normalised by $\Delta_{av}/\Delta_{max} = 1.0$, where Δ_{max} is the maximum observed weighted shift difference.[29]

We thank Thomas Scheibel, Heiko Ingo Siegmund, Kerstin Abelmann and Ralph Peteranderl for initial experiments. This work was support by grants from the DFG (SFB 594) to H.K. and J.B. and an Alexander von Humboldt fellowship to J.F.

[1] L. H. Pearl, C. Prodromou, *Adv. Protein Chem.* **2001**, *59*, 157–186.
[2] K. Richter, J. Buchner, *J. Cell. Physiol.* **2001**, *188*, 281–290.
[3] W. B. Pratt, D. O. Toft, *Endocr. Rev.* **1997**, *18*, 306–360.
[4] J. C. Young, I. Moarefi, F. U. Hartl, *J. Cell Biol.* **2001**, *154*, 267–273.
[5] B. Panaretou, C. Prodromou, S. M. Roe, R. O'Brien, J. E. Ladbury, P. W. Piper, L. H. Pearl, *EMBO J.* **1998**, *17*, 4829–4836.
[6] W. M. J. Obermann, H. Sondermann, A. A. Russo, N. P. Pavletich, F. U. Hartl, *J. Cell Biol.* **1998**, *143*, 901–910.
[7] C. Prodromou, S. M. Roe, R. O'Brien, J. E. Ladbury, P. W. Piper, L. H. Pearl, *Cell* **1997**, *90*, 65–75.
[8] K. Richter, P. Muschler, O. Hainzl, J. Buchner, *J. Biol. Chem.* **2001**, *276*, 33689–33696.
[9] C. Prodromou, B. Panaretou, S. Chohan, G. Siligardi, R. O'Brien, J. E. Ladbury, S. M. Roe, P. W. Piper, L. H. Pearl, *EMBO J.* **2000**, *19*, 4383–4392.
[10] K. Richter, J. Reinstein, J. Buchner, *J. Biol. Chem.* **2002**, *277*, 44905–44910.
[11] R. Dutta, M. Inouye, *Trends Biochem. Sci.* **2000**, *25*, 24–28.
[12] C. Ban, M. Junop, W. Yang, *Cell* **1999**, *97*, 85–97.
[13] S. V. Sharma, T. Agatsuma, H. Nakano, *Oncogene* **1998**, *16*, 2639–2645.
[14] L. Whitesell, E. G. Mimnaugh, B. Decosta, C. E. Myers, L. M. Neckers, *Proc. Natl. Acad. Sci. USA* **1994**, *91*, 8324–8328.
[15] L. Busconi, J. Z. Guan, B. M. Denker, *J. Biol. Chem.* **2000**, *275*, 1565–1569.
[16] M. O. Lee, E. O. Kim, H. J. Kwon, Y. M. Kim, H. J. Kang, J. E. Lee, *Mol. Cell. Endocrinol.* **2002**, *188*, 47–54.
[17] M. Sakagami, P. Morrison, W. J. Welch, *Cell Stress Chaperones* **1999**, *4*, 19–28.
[18] J. P. Grenert, W. P. Sullivan, P. Fadden, T. A. J. Haystead, J. Clark, E. Mimnaugh, H. Krutzsch, H. J. Ochel, T. W. Schulte, E. Sausville, L. M. Neckers, D. O. Toft, *J. Biol. Chem.* **1997**, *272*, 23843–23850.
[19] T. Weikl, P. Muschler, K. Richter, T. Veit, J. Reinstein, J. Buchner, *J. Mol. Biol.* **2000**, *303*, 583–592.
[20] S. M. Roe, C. Prodromou, R. O'Brien, J. E. Ladbury, P. W. Piper, L. H. Pearl, *J. Med. Chem.* **1999**, *42*, 260–266.
[21] C. E. Stebbins, A. A. Russo, C. Schneider, N. Rosen, F. U. Hartl, N. P. Pavletich, *Cell* **1997**, *89*, 239–250.
[22] R. M. Salek, M. A. Williams, C. Prodromou, L. H. Pearl, J. E. Ladbury, *J. Biomol. NMR* **2002**, *23*, 327–328.

[23] S. B. Shuker, P. J. Hajduk, R. P. Meadows, S. W. Fesik, *Science* **1996**, *274*, 1531 – 1534.
[24] G. Gemmecker, M. Eberstadt, A. Buhr, R. Lanz, S. G. Grdadolnik, H. Kessler, B. Erni, *Biochemistry* **1997**, *36*, 7408 – 7417.
[25] Y. Gosser, T. Hermann, A. Majumdar, W. D. Hu, R. Frederick, F. Jiang, W. J. Xu, D. J. Patel, *Nat. Struct. Biol.* **2001**, *8*, 146 – 150.
[26] C. Klein, E. Planker, T. Diercks, H. Kessler, K. P. Künkele, K. Lang, S. Hansen, M. Schwaiger, *J. Biol. Chem.* **2001**, *276*, 49 020 – 49 027.
[27] S. Mori, C. Abeygunawardana, M. O. Johnson, P. C. M. Vanzijl, *J. Magn. Reson. Ser. B* **1995**, *108*, 94 – 98.
[28] H. Lüttgen, R. Robelek, R. Mühlberger, T. Diercks, S. C. Schuster, P. Kohler, H. Kessler, A. Bacher, G. Richter, *J. Mol. Biol.* **2002**, *316*, 875 – 885.
[29] S. Grzesiek, A. Bax, G. M. Clore, A. M. Gronenborn, J. S. Hu, J. Kaufman, I. Palmer, S. J. Stahl, P. T. Wingfield, *Nat. Struct. Biol.* **1996**, *3*, 340 – 345.
[30] M. Maruya, M. Sameshima, T. Nemoto, I. Yahara, *J. Mol. Biol.* **1999**, *285*, 903 – 907.
[31] T. Scheibel, T. Weikl, J. Buchner, *Proc. Natl. Acad. Sci. USA* **1998**, *95*, 1495 – 1499.
[32] M. Salzmann, K. Pervushin, G. Wider, H. Senn, K. Wüthrich, *Proc. Natl. Acad. Sci. USA* **1998**, *95*, 13 585 – 13 590.
[33] M. Salzmann, G. Wider, K. Pervushin, H. Senn, K. Wüthrich, *J. Am. Chem. Soc.* **1999**, *121*, 844 – 848.
[34] M. Leutner, R. M. Gschwind, J. Liermann, C. Schwarz, G. Gemmecker, H. Kessler, *J. Biomol. NMR* **1998**, *11*, 31 – 43.
[35] M. Piotto, V. Saudek, V. Sklenář, *J. Biomol. NMR* **1992**, *2*, 661 – 665.
[36] V. Sklenář, M. Piotto, R. Leppik, V. Saudek, *J. Magn. Reson. Ser. A* **1993**, *102*, 241 – 245.
[37] T. D. Goddard, D. G. Kneller, University of California, San Francisco.
[38] D. G. Kneller, I. D. Kuntz, *J. Cell. Biochem. Suppl. 17 C* **1993**, 254.
[39] J. Sambrook, D. W. Russel, *Molecular Cloning Vol. 1*, Cold Spring Harbour Laboratory Press, Cold Spring Harbour, **2001**.

Received: May 14, 2003 [F 658]

